Electronic Supplementary Material (ESI) for Physical Chemistry Chemical Physics.

Electronic Supplementary Information

Quantifying ultrafast charge carrier injection from methylammonium lead iodide into the hole-transport material H101 and mesoporous TiO_2 using Vis-NIR transient absorption

Johannes R. Klein, Mirko Scholz, Kawon Oum and Thomas Lenzer**

Universität Siegen, Physikalische Chemie, Adolf-Reichwein-Str. 2, 57076 Siegen, Germany,
E-mail: oum@chemie.uni-siegen.de, lenzer@chemie.uni-siegen.de

Table of Contents

1. Photoluminescence quenching efficiency of H101

The steady-state photoluminescence (PL) of the samples was recorded on an Agilent Cary Eclipse spectrometer as described in our previous publications.[1,2] Four MAPI samples were prepared on mesoporous TiO_2 to determine the PL quenching efficiency. Photos of typical MAPI samples are depicted in Fig. S1. Steady-state absorption and PL spectra for the samples without H101 are shown as dotted lines in Fig. S2. Stray light contributions were subtracted from the PL spectra before integrating them over the range 12000-14250 cm^{-1}. After coating the samples with H101, the second set of spectra, shown as solid lines, were obtained, and the PL intensity was integrated in the same way. The results are presented in Table S1. Coating the perovskite samples by H101 reduces the PL intensity to (23.7 ± 5.3)% of the initial value. The lower absorption signal between 480 and 650 nm of the H101-coated samples arises from a decrease in surface reflectance, as discussed below. The additional absorption contribution of H101 around 400 nm is clearly observed.

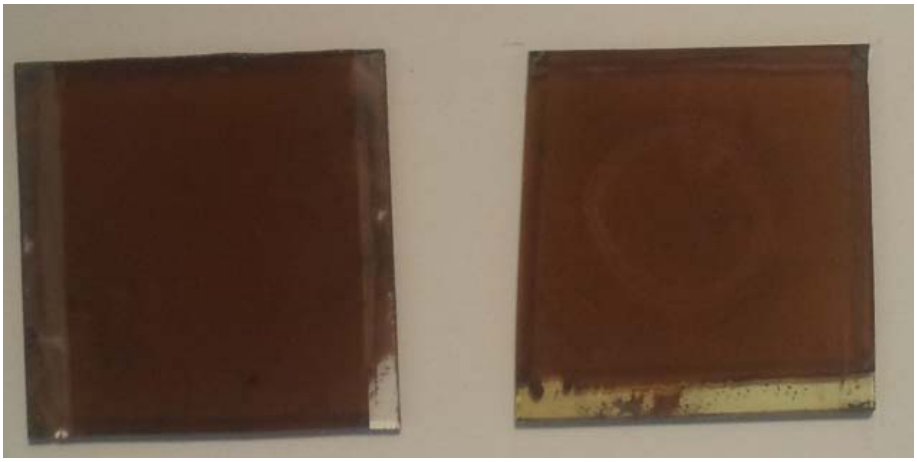

Figure S1. Photos showing representative samples of MAPI on mesoporous TiO_2 without (left) and with an additional layer of the hole transport material H101 (right).

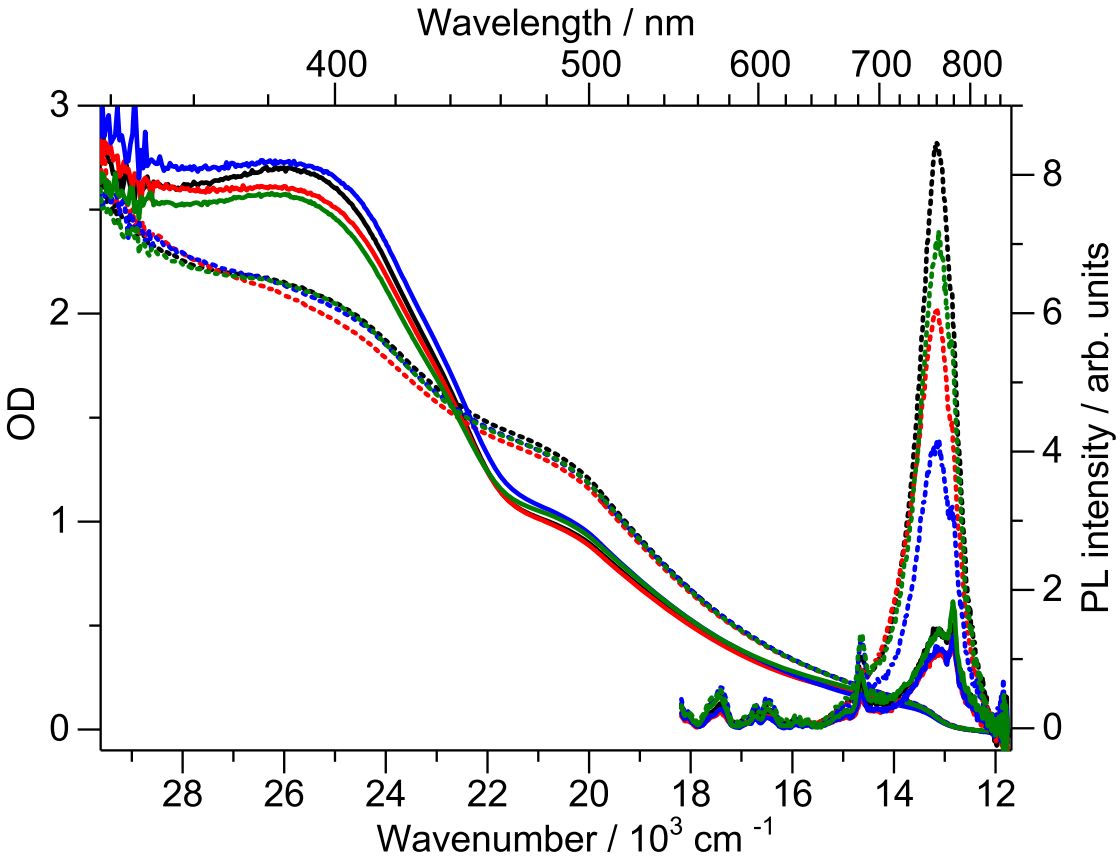

Figure S2. Steady-state absorption spectra (left) and photoluminescence spectra (right) of four different MAPI samples (black, red, green and blue lines) without and with an additional H101 HTM layer (dotted and solid lines, respectively). The PL signals were corrected for the stray light of the excitation source. PL excitation wavelength: 500 nm.

Table S1. PL intensities integrated over the range 12000-14250 cm^{-1} of four MAPI samples on mesoporous TiO_2 without (I_{PL}) and with an H101 HTM layer (I_{PL}(H101)) and the respective PL ratios.

Sample	I_{PL} (arb. units)	I_{PL}(H101) (arb. units)	I_{PL}(H101)/I_{PL} (%)
1	81.41	15.98	19.6
2	63.41	12.72	20.1
3	42.18	13.13	31.1
4	69.83	16.83	24.1
		Mean	**23.7**
		σ	**5.3**

2. Addition of an organic top layer to glass-TiO_2-MAPI

Steady-state absorption spectra of the thin films were recorded in a nitrogen atmosphere with illumination from the glass side. As shown in the main manuscript, we observed a reduction in the optical density of the thin films when either PMMA or H101 layers were coated onto the glass-TiO_2-MAPI architecture (Fig. 4). In the following we consider the addition of a PMMA layer, because accurate refractive index data are available for this material. In that case, the N_2-MAPI interface is exchanged by the two interfaces N_2-PMMA and PMMA-MAPI. The interfaces N_2-glass and glass-MAPI remain unchanged and are not considered further.

The reflectance R at the boundary of two materials for radiation striking the interface at normal incidence was calculated using Fresnel's law: $R = ([n_1(\lambda)-n_2(\lambda)]/[n_1(\lambda)+n_2(\lambda)])^2$.[3] The wavelength-dependent refractive indices $n_1(\lambda)$ and $n_2(\lambda)$ for N_2, MAPI and PMMA were taken from the refractive index data base.[4-6] For the sake of simplicity we neglected thin-layer interference effects (resulting in weak periodic modulations in the spectra) and the different scattering properties of the non-ideal interfaces produced by spin-coating.

Figure S3(a) shows the calculated reflectance for the different interfaces in the wavelength region of interest. The reflectance of the N_2-MAPI interface (red line) is higher than the summed reflectance of the N_2-PMMA and PMMA-MAPI layers (magenta line). As a result, coating with PMMA (and also H101) will reduce the reflectance ($\Delta R < 0$, blue line) and will lead to a reduction of the OD of the thin film. This is demonstrated in Fig. S3(b). The experimentally measured OD of the film without PMMA (red line) is larger than the one with PMMA (black line). The calculated absorption spectrum with PMMA (panel (b), blue line) was obtained by correcting the experimental absorption spectrum without PMMA (panel (b), red line) for the calculated change in reflectance (panel (a), blue line). It reproduces the experimental absorption spectrum (panel (b), black line) quite well, but the calculated OD reduction is somewhat too large. The difference is likely due to the increased scattering introduced by the additional PMMA layer which was not considered in the calculation. Furthermore, an underlying wavelength-dependent modulation due to interference effects of the added PMMA layer, which was also not considered in the calculation, will contribute to the deviations. Still the main effect of the reduction in reflectance upon adding PMMA is nicely reproduced even using this simple approach.

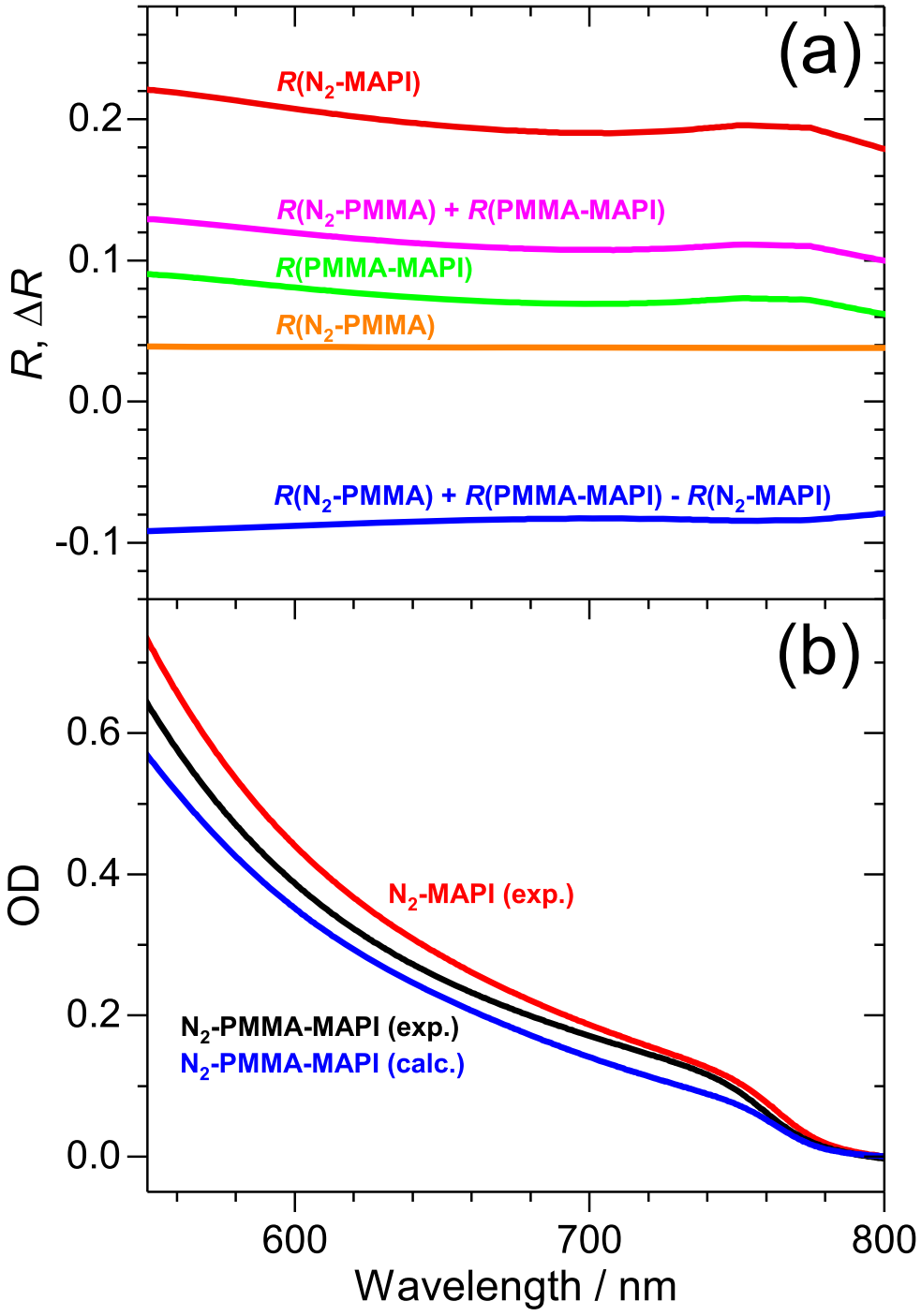

Figure S3. (a) Reflectance R and change in reflectance ΔR for different interfaces and different combinations of interfaces involving MAPI, (b) optical density of different MAPI thin films: N_2-MAPI interface (red line: experimental spectrum) and N_2-PMMA-MAPI interfaces (black line: experimental spectrum, blue line: calculated spectrum).

3. Spectroelectrochemistry experiments

Spectroelectrochemistry experiments were carried out to obtain steady-state absorption spectra of the cation species using a setup described previously.[7,8] Figures S4 and S5 show cyclic voltammograms for H101 in acetonitrile and the corresponding potential-dependent difference absorption spectra. One-electron oxidation of H101 results in formation of the radical cation $H101^{\bullet+}$, with two characteristic absorption peaks at 635 and 1470 nm (Fig. S5, 0.6 V, blue line). At higher voltage, $H101^{\bullet+}$ is oxidised further to the dication $H101^{2+}$ featuring a prominent single peak at 1000 nm (Fig. S5, 1.2 V, red line).

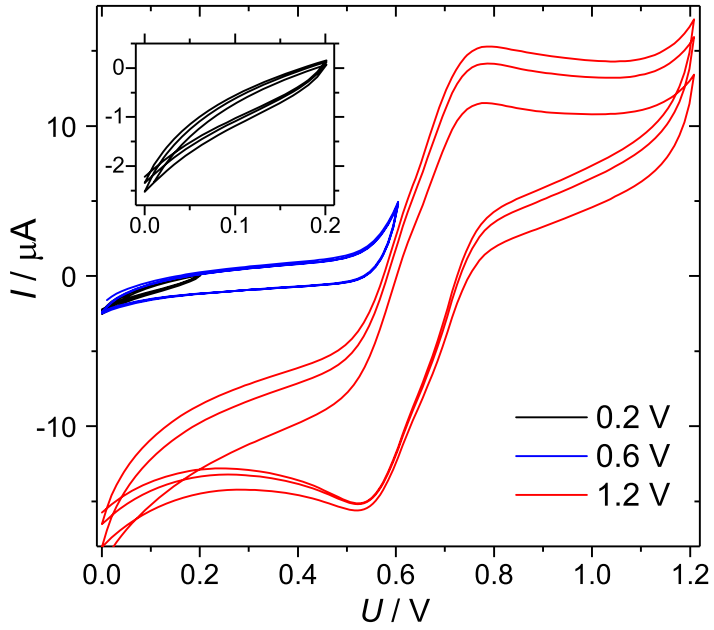

Figure S4. Cyclic voltammograms of H101 in acetonitrile at different voltages using a scan rate of 0.1 V s^{-1}.

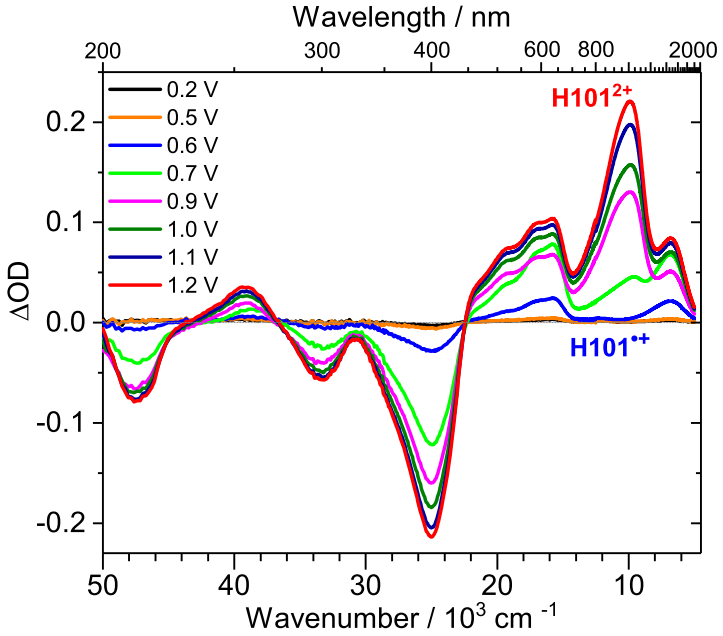

Figure S5. Difference absorption spectra from spectroelectrochemistry at different voltages.

4. Biexponential fits of the NIR kinetics at 1500 nm

Figure S6 shows the biexponential fits of the transient absorption kinetics at 1500 nm for different geometries and wavelengths of the excitation beam, *i.e.* panels (a)-(f) correspond to the conditions (A)-(F) in Table 1 and Fig. 9 of the main manuscript.

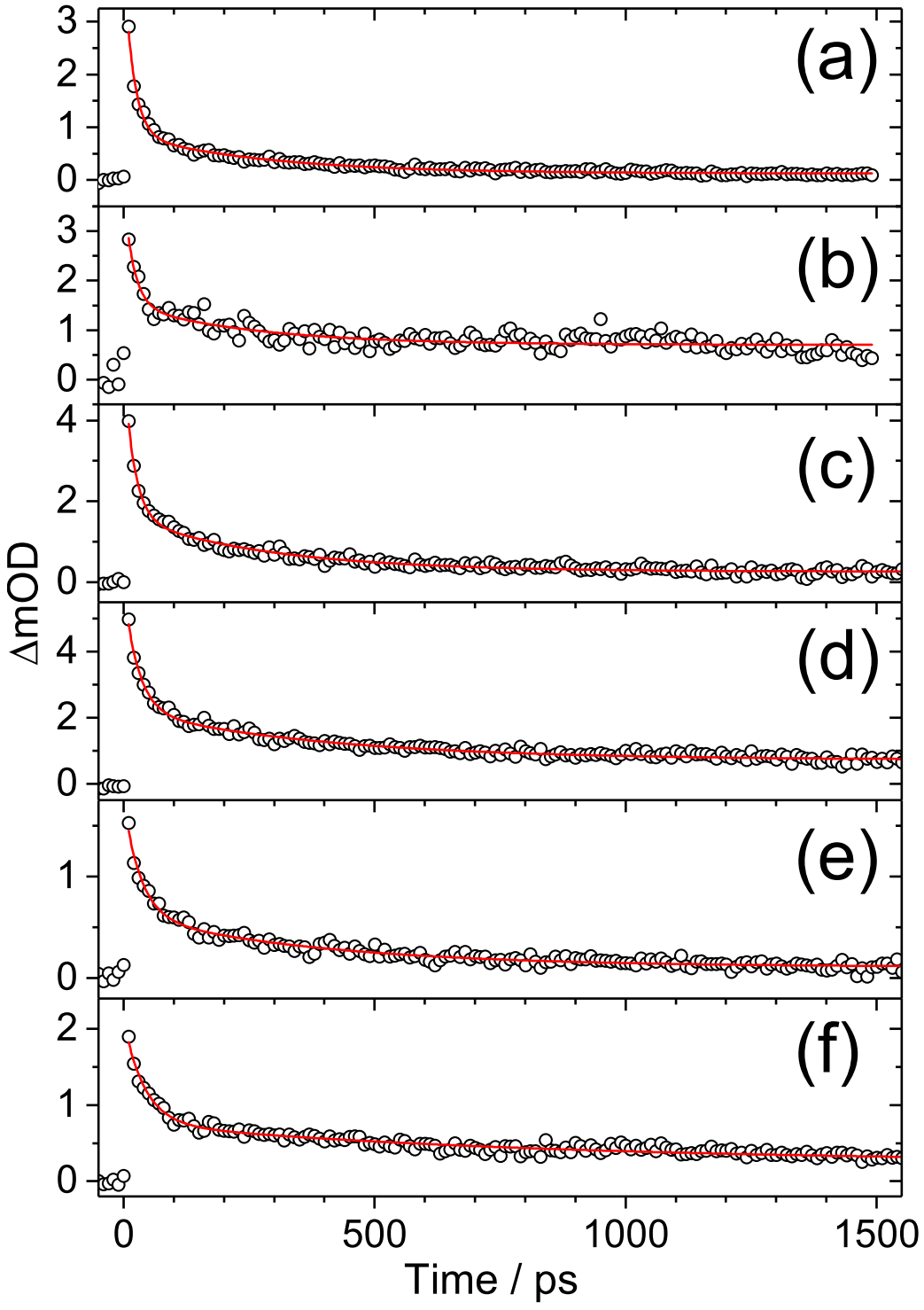

Figure S6. Transient absorption kinetics at 1500 nm including fit lines. Kinetic traces in panels (a)-(f) correspond to conditions (A)-(F) in Table 1 and Fig. 9 of the main manuscript.

5. References

1. O. Flender, J. R. Klein, T. Lenzer and K. Oum, *Phys. Chem. Chem. Phys.*, 2015, **17**, 19238.
2. J. R. Klein, O. Flender, M. Scholz, K. Oum and T. Lenzer, *Phys. Chem. Chem. Phys.*, 2016, **18**, 10800.
3. H. J. Kuhn, S. E. Braslavsky and R. Schmidt, *Pure Appl. Chem.*, 2004, **76**, 2105.
4. M. Polyanskiy, https://refractiveindex.info/2017.
5. E. R. Peck and B. N. Khanna, *J. Opt. Soc. Am.*, 1966, **56**, 1059.
6. L. J. Phillips, A. M. Rashed, R. E. Treharne, J. Kay, P. Yates, I. Z. Mitrovic, A. Weerakkody, S. Hal and K. Durose, *Sol. Energy Mater. Sol. Cells*, 2016, **147**, 327.
7. K. Oum, P. W. Lohse, J. R. Klein, O. Flender, M. Scholz, A. Hagfeldt, G. Boschloo and T. Lenzer, *Phys. Chem. Chem. Phys.*, 2013, **15**, 3906.
8. O. Flender, M. Scholz, J. R. Klein, K. Oum and T. Lenzer, *Phys. Chem. Chem. Phys.*, 2016, **18**, 26010.